ACS Chemical Neuroscience

Research Article

pubs.acs.org/chemneuro

Multiple Function Fluorescein Probe Performs Metal Chelation, Disaggregation, and Modulation of Aggregated Aβ and Aβ-Cu Complex

B. Muthuraj,[†] Sourav Layek,[‡] S. N. Balaji,[‡] Vishal Trivedi,*[,‡] and Parameswar Krishnan Iyer*[,†]

[†]Department of Chemistry, and [‡]Department of Biosciences and Bioengineering, Indian Institute of Technology Guwahati-781039, Assam, India

Supporting Information

ABSTRACT: An exceptional probe comprising indole-3-carboxaldehyde fluorescein hydrazone (FI) performs multiple tasks, namely, disaggregating amyloid β (Aβ) aggregates in different biomarker environments such as cerebrospinal fluid (CSF), Aβ1−40 fibrils, β-amyloid lysozyme aggregates (LA), and U87 MG human astrocyte cells. Additionally, the probe FI binds with Cu^{2+} ions selectively, disrupts the Aβ aggregates that vary from few nanometers to micrometers, and prevents their reaggregation, thereby performing disaggregation and modulation of amyloid-β in the presence as well as absence of Cu^{2+} ion. The excellent selectivity of probe FI for Cu^{2+} was effectively utilized to modulate the assembly of metal-induced Aβ aggregates by metal chelation with the "turn-on" fluorescence via spirolactam ring opening of FI as well as the metal-free Aβ fibrils by noncovalent interactions. These results confirm that FI has exceptional ability to perform multifaceted tasks such as metal chelation in intracellular conditions using Aβ lysozyme aggregates in cellular environments by the disruption of β-sheet rich Aβ fibrils into disaggregated forms. Subsequently, it was confirmed that FI had the ability to cross the blood-brain barrier and it also modulated the metal induced Aβ fibrils in cellular environments by "turn-on" fluorescence, which are the most vital properties of a probe or a therapeutic agent. Furthermore, the morphology changes were examined by atomic force microscopy (AFM), polarizable optical microscopy (POM), fluorescence microscopy, and dynamic light scattering (DLS) studies. These results provide very valuable clues on the Aβ (CSF Aβ fibrils, Aβ1−40 fibrils, β-amyloid lysozyme aggregates) disaggregation behavior via in vitro studies, which constitute the first insights into intracellular disaggregation of Aβ by "turn-on" method thereby influencing amyloidogenesis.

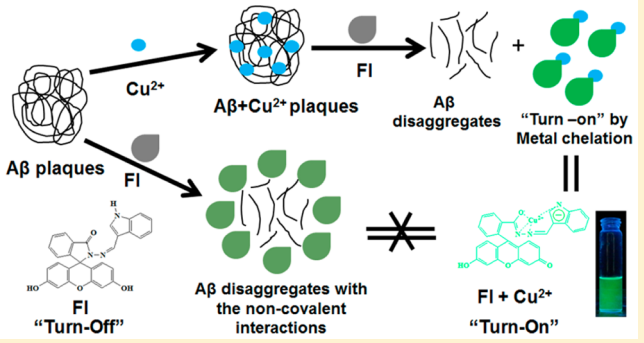

KEYWORDS: *Amyloid β, Alzheimer's disease, cerebrospinal fluid, neurodegenerative diseases, fluorescein, therapeutics, aggregation, modulator*

Alzheimer's disease (AD), the most prevalent cause of dementia among elderly population, affects >40 million people worldwide.[1,2] Early symptoms such as difficulty to remember newly acquired information and other severe symptoms such as mood and behavior changes, perplexity, severe memory loss, and judgment alteration coupled with difficulties in speaking, writing, and walking predominantly begin to appear with aging. As per the AD hypothesis, the aggregation of amyloid-β (Aβ) peptide is linked to the etiology of the disease, since soluble monomeric forms are found in the healthy brain while amyloid plaques are detected in an AD patient's brain.[3,4] These micrometer sized aggregates provide an important pharmacological target in the ability of drugs to (a) disrupt the already formed Aβ aggregates, (b) prevent Aβ aggregation, or (c) be capable of arresting and inverting the progression of AD.[5,6] Aβ40 and Aβ42 peptides are the primary species in the structure of the senile plaques found in the brain tissues of AD patients.[6−8] Metal ions, such as iron, copper, and zinc, are known to interact with Aβ peptides and promote their aggregation as well as generation of neurotoxicity.[9−18] They also have the ability to modulate the aggregation of Aβ peptides as observed by in vitro experiments.[9,19−22] Despite being an important pharmacological target for AD pathogenesis, separation of toxic metals from Aβ peptide fibrils along with their disruption and modulation remains unresolved.

The accumulation of metals such as iron, copper, and zinc within the senile plaques can reach levels of up to 400, 950, and 1100 mm, respectively, which is 3−5 times higher in concentration as compared to healthy brain.[23−27] To reduce the harmful effects of excess metal deposition, newer therapies that focus on metal ion chelation for AD are being developed.[28−30] Metal chelators are potential therapeutic prospects due to the metal ion hypothesis and the possible

Received: July 29, 2015
Revised: September 1, 2015
Published: September 2, 2015

DOI: 10.1021/acschemneuro.5b00205
ACS Chem. Neurosci. 2015, 6, 1880−1891

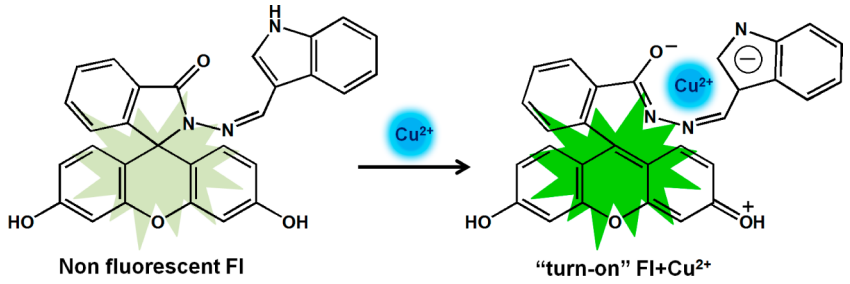

Figure 1. Nonfluorescent FI (3 μM) selectively detects Cu^{2+} ion (3 equiv) in HEPES buffer solution (pH 7.4, 10 mM).

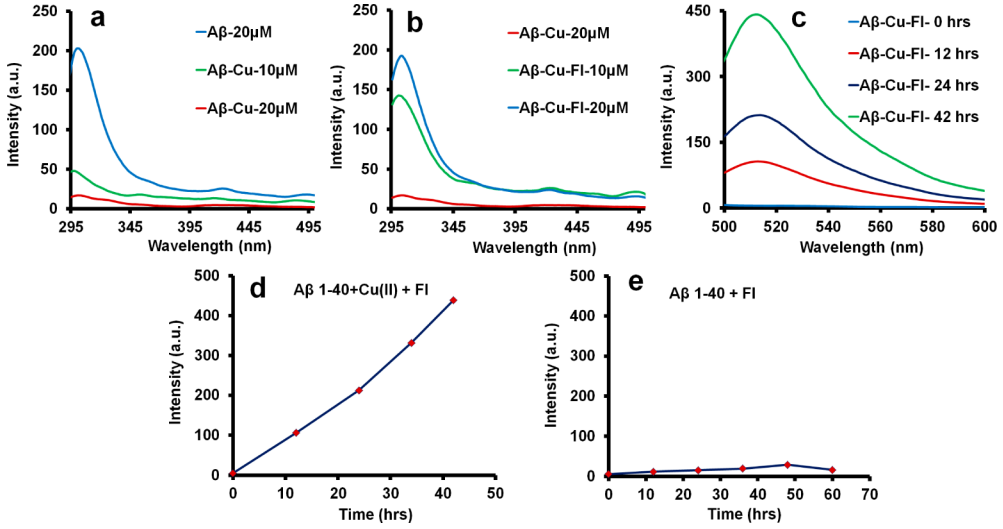

Figure 2. (a) Tyr fluorescence quenching in Aβ1−40 (20 μM), 10 mM HEPES buffer (pH 7.4) upon the addition of 10 and 20 μM Cu^{2+}. (b) Tyr fluorescence dequenching upon the addition of 10 and 20 μM FI into Aβ1−40−Cu^{2+} (1:1) in 10 mM HEPES buffer (pH 7.4). (c) At excitation of 465 nm, the emission peak is obtained at 518 nm for FI−Cu^{2+} (0−42 h). (d) Modulation or disaggregation of Aβ1−40−Cu^{2+} aggregates by FI: Fluorescent changes of Aβ1−40−Cu^{2+} (20 μM) aggregates with FI (20 μM) were monitored with different time incubations at 465 nm excitation, the "turn-on" fluorescent enhancement peak is obtained at 518 nm for FI−Cu^{2+} complex. (e) Modulation or disaggregation of Aβ1−40 aggregates by FI: Fluorescent changes of Aβ1−40 (20 μM) aggregates with FI (20 μM) were monitored with different time incubations at 465 nm excitation; no significant "turn-on" fluorescent enhancement peak is obtained at 518 nm.

contribution of metal−Aβ to AD. For therapeutic strategy, a new type of compound based on inhibiting or modulating metal−Aβ interactions, known as metal−protein attenuating compounds (MPACs), are being designed and developed. Compared with traditional chelators such as DFO and TETA, there are two metal chelators which have accomplished phase II clinical trials like clioquinol (CQ) and its derivative (PBT2) that have been tested in murine AD models and AD patients.[31,32] The hydroxyquinoline derivatives of clioquinol (CQ) decreased Aβ aggregates and showed improved cognition in phase II clinical trials for AD due to its ability to inhibit binding of Cu(II) to Aβ via chelation.[31,33,34] In addition, derivatives of 8-hydroxyquinoline ionophore PBT2 also resulted in improved cognition ability (learning and memory) by redistributing Cu(II) and Zn(II) and by lowering CSF levels of Aβ in phase II clinical trials.[35,36] Both, CQ and PBT2 have the ability to alter the metal levels as well as the Aβ clearance. Hence, newer and appropriate efforts are necessary for developing efficient molecules for targeting metal−Aβ species and to overcome this challenge posed by both metals as well as self-assembled peptides.[37−41] To study this relation between metal−Aβ complexes with AD pathology, it is necessary to design and synthesize molecules with multifunctional ability.[42−45] The potential development of metal chelating molecules and AD therapy could help in understanding the importance of fundamental mechanisms involving Cu(II) binding with Aβ peptide and the successful implementation of this strategy could guide the aspect of metal−Aβ-induced aggregation and disaggregation.

The Aβ1−40 peptide contains several binding sites with the hydrophilic N-terminal amine, three His moieties at 6, 13, and 14 as well as four carboxylic acid moieties at 1, 3, 7, and 11.[46] The hydrophilic N-terminal part of Aβ1−40 is responsible for binding the metal ions, namely, copper, zinc, and iron, which are accountable for the modulation of Aβ aggregation and neurotoxicity.[5] The redox active metal ions and cofactors (heme) bind Aβ peptides and can produce harmful and partially reduced oxygen species (PROS) under physiological conditions.[47−49] They also lead to the formation of soluble cross-linked dimeric species of Tyr10 repeatedly by oxidization of the Aβ peptide side chains.[50,51] This process further leads to the formation of Aβ aggregates responsible for progressive neurodegeneration in AD. Tyrosine (Tyr) is a crucial amino acid for both conformation as well as probing the biological activity of Aβ due to its emission in the visible region.[52−55] Thus, to conform the binding of copper in Aβ peptide, the fluorescence of Tyr was carefully followed, since its fluorescence is quenched on binding Cu^{2+}, whereas the fluorescence is retained on withdrawal of Cu^{2+} from Aβ peptide.[56]

DOI: 10.1021/acschemneuro.5b00205
ACS Chem. Neurosci. 2015, 6, 1880−1891

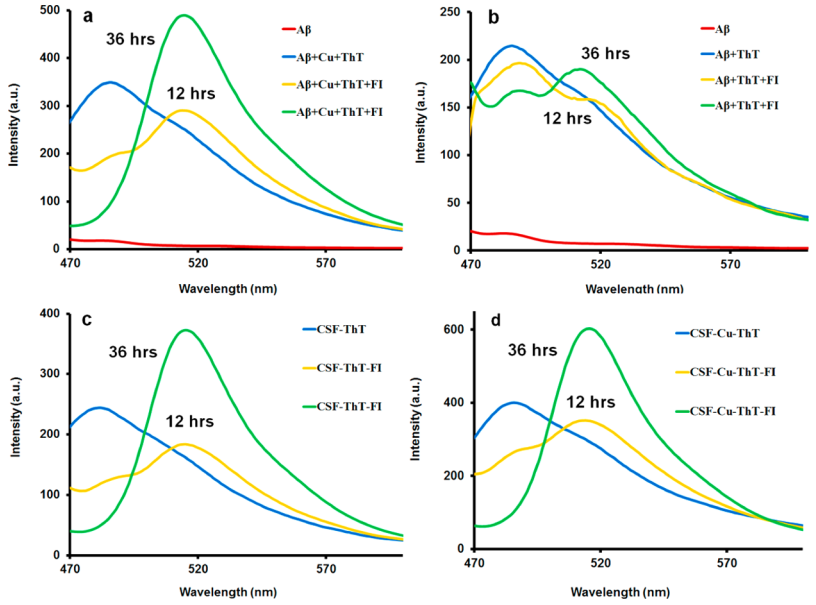

Figure 3. (a) Aggregation of Aβ1−40 with Cu^{2+} in the presence of ThT and disaggregation of Aβ1−40−Cu^{2+} in the presence of FI. (b) Aggregation of Aβ1−40−ThT emission peak at 487 nm shows insignificant change on adding FI. (c, d) CSF aggregates in the absence and presence of Cu^{2+} ion with ThT (pH 7.4 in 10 mM HEPES) showed emission peak at 487 nm (λ_{ex} 440 nm) and disaggregation of CSF Aβ aggregates observed in the presence of FI (λ_{ex} 440 nm, 31 nm shifted to 518 nm with FI).

RESULT AND DISCUSSION

The indole-3-carboxaldehyde fluorescein hydrazone probe (FI) synthesized in high yields (Figure 1)[57] was selected as a modulator or anti-AD molecule, since it possesses several exceptional properties such as easy synthesis, very high aqueous solubility, easy cell penetrability, high fluorescence quantum yield, high molar extinction coefficient value, and most importantly a biofriendly nontoxic fluorophore for the highly selective "turn-on" detection of Cu^{2+} ion. Hence, the modulation or disaggregation of Aβ peptides, such as Aβ fibrils (with and without Cu^{2+}) and Aβ aggregates in real CSF and β-amyloid lysozyme aggregates (LA) (with and without Cu^{2+}), were studied in the presence of multifunctional FI to control the AD progression as well as to develop a method that could lead to the design and development of better therapeutic alternatives for efficient control and prevention of AD.

Tyrosine Intrinsic Fluorescence Assay. Since Tyr10 is located in the close proximity to the three histidine residues (6, 13, 14), it is expected to be involved in metal coordination, thereby resulting in metal-induced chemical changes.[58] Tyr10 is the main fluorophore for the intrinsic fluorescence of Aβ1−40 and has been utilized to investigate the formation of a complex between Aβ1−40 and Cu^{2+} ions.[59−62] The tyrosine intrinsic fluorescence of Aβ1−40 is quenched when Cu^{2+} ion binds to the Aβ1−40 peptide, whereas the fluorescence is regained on adding Cu^{2+} ion chelators (FI).[60−64] This transformation in the tyrosine intrinsic fluorescence assay was utilized to exploit the capability of FI for chelating Cu^{2+} ions from Aβ1−40−Cu^{2+}aggregates.

The modifications in the fluorescence of Tyr10 (in Aβ1−40 sequence) were monitored (Figure 2) by adding 10 and 20 μM Cu^{2+} to 20 μM Aβ1−40 in 10 mM HEPES buffer (pH 7.4). On adding 10 μM concentration of Cu^{2+} ions into the Aβ1−40 solution, the fluorescence quenching of Tyr10 at 305 nm (Figure 2a, blue line) occurs rapidly due to the formation of Aβ1−40−Cu^{2+} complex with the three His moieties at 6, 13, and 14 as well as four carboxylic acid moieties at 1, 3, 7, and 11. Further addition of up to 20 μM Cu^{2+} to Aβ1−40 solution resulted in nearly complete quenching of Tyr10 fluorescence (Figure 2a, green and red lines).[65] The fluorescence quenching of Tyr10 occurred due to the significant increase in the electron density at the Cu^{2+} center which further results in the charge transfer to other groups in close proximity such as Tyr10 residue. This interaction was expected to reduce the fluorescence intensity upon Cu^{2+} binding by facilitating nonradiative energy transfer from the excited state of Tyr10.[58]

Metal Chelation from Aβ1−40−Cu^{2+} Aggregates Using FI Chelator. After 24 h incubation of the Aβ1−40−Cu^{2+} complex, the probe FI was utilized to monitor the chelation of Cu^{2+} from the complex of Aβ1−40−Cu^{2+} aggregates. The quenched intrinsic fluorescence of Tyr regained rapidly upon addition of FI (20 μM). The resulting enhanced fluorescence intensity was compared with the fluorescence intensity of Aβ−Cu^{2+} alone to determine whether FI (as chelator) could extract copper and/or modulate Aβ1−40−Cu^{2+} aggregates (Figure 2b). In a typical experiment, the addition of up to 20 μM FI to Aβ1−40−Cu^{2+} aggregates resulted in the Tyr fluorescence being regained completely (without incubation) since the interactions between Cu^{2+} and Tyr OH were disrupted (Figure 2b). To further validate the role of Cu^{2+} ions in Aβ1−40, the Aβ−Cu−FI complex was excited at 465 nm (0−42 h time incubations), resulting in a new and prominent emission peak at 518 nm (Figure 2c, d) corresponding to the formation of FI−Cu^{2+} complex (Figure 1). When excited at 465 nm, Aβ−Cu−FI did not show any emission in the range of 500−600 nm at 0 h (Figure 2c, light blue line), indicating that FI remains in spirolactam ring form but disrupts the Tyr OH interactions with Cu^{2+} ions. After incubation (0−42 h), when the Aβ−Cu−FI complex was excited at 465 nm, Cu^{2+} induced the spirolactam ring opening of FI with a significant "turn-on" fluorescence response at 518 nm and a highly bright green fluorescence (Figure 2c, d; 0−42 h) was observed. The apparent binding constant for the formation of the respective complexes was evaluated using the Benesi−Hildebrand (B−H)

DOI: 10.1021/acschemneuro.5b00205
ACS Chem. Neurosci. 2015, 6, 1880−1891

plot and was estimated to be 6.33×10^4 M^{-1} by the emission spectral changes at 518 nm (Figure S1). However, in the present study, the probe FI had a major influence on the Tyr fluorescence of Aβ1−40−Cu^{2+} aggregates (Figure 2b). These results indicate that FI was able to chelate metal ions from metal-bound Aβ species to different extents. When similar experiments were performed with FI (20 μM) and Aβ self-aggregates (without Cu^{2+}), no significant "turn-on" fluorescence response at 518 nm (Figure 2e, 0−60 h) occurred. Moreover, we also performed control experiments to chelate metal ion from Aβ1−40 (20 μM) + Cu^{2+} (20 μM) aggregates by nonfluorescent metal chelator (EDTA 2 equiv), while monitoring Tyr fluorescence at 305 nm. No significant dequenching was observed by EDTA (Figure S2) as compared to the probe FI which confirms that FI has a stronger affinity for Cu^{2+} as compared to Aβ1−40. Thus, the probe FI could retrieve Cu^{2+} from Aβ1−40 and modulate the Aβ aggregates. Finally, these studies confirm the superiorr performance of FI as compared to the previously reported metal chelators.[66−70]

Thioflavin T (ThT) Assay. ThT is one of the most widely used fluorescent dyes to identify Aβ fibrils.[71,72] A gradual enhancement of emission peak at 487 nm (Figure S3a) occurred (0−40 h incubation time, λ_{ex} 440 nm) on addition of monomer Aβ1−40 to ThT (20 μM), signifying the formation of Aβ fibrils. The fluorescence intensity of ThT increased on binding Aβ fibrils due to the changes in the rotational freedom of the C−C bonds between the benzothiazole and aniline rings.[73] On monitoring the ThT assay in the presence of Cu^{2+} ions, the emission peak enhancement (487 nm) saturated after 12 h, which confirmed the formation of metal induced Aβ aggregates (Figure S3b). The formation of Aβ1−40 aggregates in the absence of Cu^{2+} was lesser (Figure S3a) compared to that in the presence of Cu^{2+}.[73−75] The presence of Aβ fibrils in CSF was also confirmed by ThT fluorescence enhancement (487 nm; Figure S3c).[76]

The Aβ peptide monomers are known to be less toxic.[9−18] When Cu^{2+} ions interact with Aβ peptides, they promote their aggregation into neurotoxic Aβ fibrils.[9−18] Hence, the modulation and disruption of metal-Aβ interaction can significantly influence the AD progression. To establish this metal chelation behavior and disaggregation of Aβ fibrils by FI, *in vitro* experiments using ThT assay (Figure 3) were performed. Probe FI containing Cu−Aβ1−40 complex was 31 nm red-shifted from the 487 nm emission peak of Aβ-ThT to 518 nm (which is the emission peak of FI−Cu^{2+} complex) after 12 and 36 h incubation at 37 °C (Figure 3a, orange and green lines). This 31 nm red-shifted emission once again confirms that probe FI has the ability to chelate Cu^{2+} ions from the complex of Cu−Aβ1−40 aggregated fibrils. This result also strongly supports the metal chelation hypothesis which confirms that trapping Cu^{2+} ion from aggregated Aβ1−40−Cu^{2+} complex using FI frees the ion binding sites of Aβ1−40 peptides and modulates the Cu^{2+} induced Aβ1−40 aggregation. Further, the probe FI with Aβ1−40 self-aggregates also showed a new emission peak at 518 nm with the emission of Aβ-ThT at 487 nm after 12 and 36 h incubation at 37 °C (Figure 3b, orange and green lines) which was less prominent as compared to that occurring in the presence of Cu^{2+} due to the noncovalent interactions between FI and Aβ fibrils, namely, H-bonding or weak aromatic interactions.[77−79] Furthermore, we performed additional control experiments to disaggregate Aβ1−40−Cu^{2+} aggregates by nonfluorescent metal chelator (EDTA 20 μM), while monitoring the ThT fluorescence at 487 nm, which showed ∼20% quenching by EDTA (Figure S4) that was insignificant as compared to the probe FI since FI showed "turn-on" red-shifted emission at 518 nm on metal chelation.

CSF is one of the main pathological biomarkers produced in the brain and analyzed routinely for neurological disorders.[80−83] Hence, CSF samples were evaluated to ascertain the presence of Aβ and metal deposits in it and further examine the practical role of FI in the homeostasis process. This experiment was designed to find a superior approach to disaggregate the β-sheets rich Aβ aggregates and also to prevent their reaggregation. Since these experiments were performed using real CSF samples, we tested the Aβ peptide aggregation and the presence of fibrils in it by ThT fluorescence enhancement study in the absence and presence of Cu^{2+} (Figure 3c, d, blue lines). The CSF samples were confirmed to have aggregated fibrils (Figure 3c, blue line and S3c).[76] On addition of external Cu^{2+} (20 μM) (incubation for 12 h), the emission peak at 487 nm enhanced significantly (Figure 3d, blue line) due to the formation of excess Aβ aggregation in the presence of Cu^{2+}. When FI was added into CSF−Cu^{2+} complex in the presence of ThT, the emission peak at 487 nm was red-shifted by 31 to 518 nm which is the emission peak of FI−Cu^{2+} complex (Figure 3d orange and green lines correspond to 12 and 36 h).

These results validate the multiple ability of probe FI to strongly chelate the Cu^{2+} ion present within the CSF−Cu complex as well as disaggregate the Aβ fibrils (Figure 3d). The FI mixed real CSF (without external Cu) sample also showed the emission peak at 487 nm corresponding to Aβ−ThT. This 487 nm peak was also 31 nm red-shifted to 518 nm as above, which is the emission peak of FI−Cu complex due to the likely presence of Cu^{2+} ions in the real CSF sample and their chelation by FI (Figure 3c, orange and green lines correspond to 12 and 36 h). Thus, multiple tasks such as modulation of Aβ peptides, disaggregation or disruption of Aβ fibrils by abstracting Cu^{2+} ion from CSF, and preventing them from reaggregating was demonstrated with FI and which has not been perceived to date with any other class of probes or materials. Further, this small molecule probe FI along with ThT was also screened to identify newer lead compounds that could modify the Aβ−Cu aggregates or Aβ self-aggregates. In order to determine the influence of FI binding with Aβ−Cu aggregates and Aβ self-aggregates, the fluorescence changes of ThT in the presence of Aβ−Cu aggregates and Aβ self-aggregates with FI (Figure 3) were monitored. Notably, the ThT fluorescence intensity with FI in the presence of Aβ−Cu aggregates is much lower than that without FI and/or Aβ self-aggregates with FI (Figure 3). After 36 h incubation of FI with Aβ-Cu aggregates and ThT, followed by excitation at 440 nm, the ThT emission maximum at 487 nm disappeared since there was a strong FI emission at 518 nm (Figure 3) due to the metal chelation as well as by the consistent energy transfer from donor ThT to acceptor FI (FRET).[84] The spectral overlap was confirmed from the emission spectra of ThT dye in the presence of Aβ-Cu aggregates and the excitation spectra of FI (Figure S5). Finally, the observed spectral overlap results confirm that the "turn-on" fluorescence or red-shifted emission band appearing at 518 nm were due to the formation of FI−Cu^{2+} complex (Figure S5).[84] Similarly, the experiment was also repeated with Aβ self-aggregates by following ThT fluorescence with FI. When the Aβ self-aggregate was incubated with FI in the presence of ThT and excited at 440 nm, the ThT emission maximum at 487 nm does not disappear like in the case of Aβ-Cu aggregates, but the

DOI: 10.1021/acschemneuro.5b00205
ACS Chem. Neurosci. 2015, 6, 1880−1891

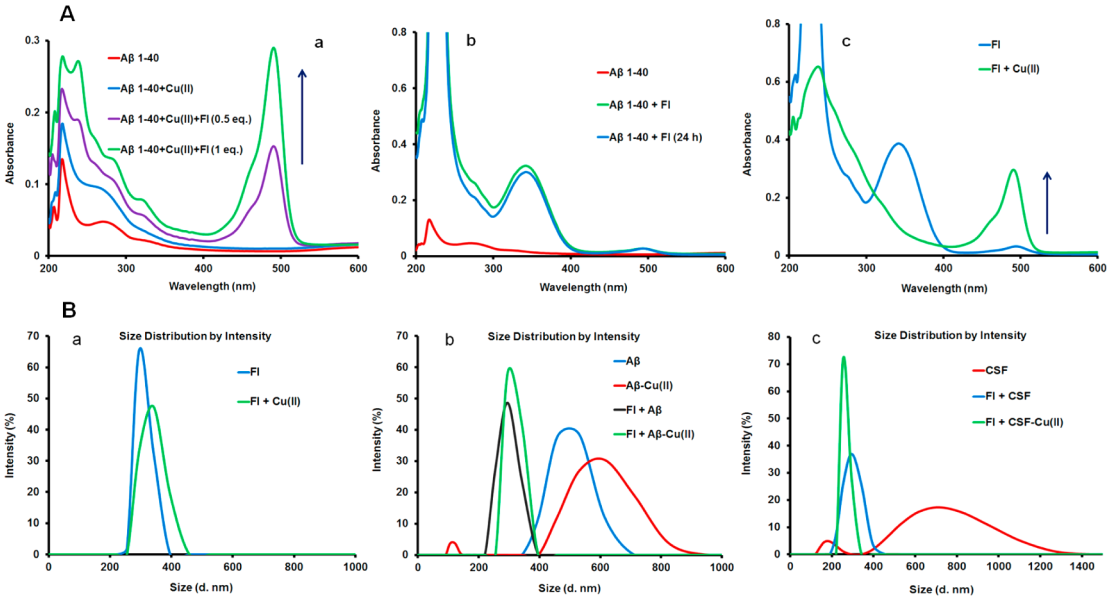

Figure 4. (A) Modulation or disaggregation of Aβ1−40−Cu^{2+} aggregates by FI: (a) UV−vis spectra of Aβ1−40 (20 μM) (red curve) and the formation of Aβ1−40−Cu^{2+} aggregates in the presence of Cu^{2+} (20 μM) (blue curve). Disaggregation of Aβ1−40−Cu^{2+} aggregates with FI (0.5 and 1 equiv) was monitored using UV−vis spectra after 24 h incubation time, with the appearance of new "turn-on" enhancement peak obtained at 492 nm. (b) UV−vis spectra of Aβ1−40 (20 μM) (red curve) and the changes of Aβ1−40 aggregates with FI (1 equiv) were monitored by using UV−vis spectra after 0 (green curve) and 24 h (blue curve) incubation time, and no significant changes were obtained at 492 nm. (c) UV−vis spectra of FI (20 μM) (blue curve) and the formation of FI−Cu^{2+} complex in the presence of Cu^{2+} (20 μM) (green curve) showed the appearance of a new "turn-on" enhancement peak obtained at 492 nm after 24 h incubation time. (B) (a) Hydrodynamic particle size (d, nm) of the molecular species of FI and FI−Cu^{2+} complex was determined by dynamic light scattering. (b, c) Hydrodynamic particle size (d, nm) of the aggregated Aβ peptides (Aβ 1−40, CSF) and disruption or disaggregation of Aβ peptides (Aβ 1−40, CSF) in the absence and presence of Cu^{2+} with and without FI in aqueous solution measured by dynamic light scattering.

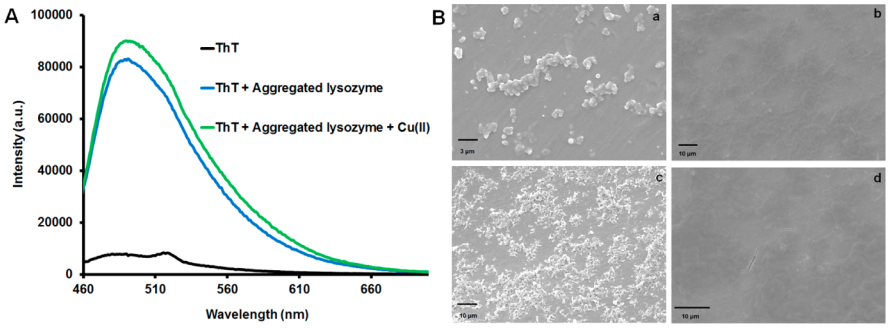

Figure 5. (A) Lysozyme aggregated amyloid fibrils and plaques in the absence and presence of Cu^{2+} with ThT (pH 7.4 in PBS) showed emission peak (blue line) at λ_{em} 487 nm (λ_{ex} 440 nm). (B) (a, c) SEM images of the morphologies of lysozyme aggregated fibrils (absence of Cu^{2+} ion) and aggregated amyloid plaques in the presence of copper ions (20 μM). (b, d) Lysozyme aggregated fibrils and aggregated amyloid plaques are disaggregated in the presence of modulator FI (20 μM).

energy transfer from donor of ThT to acceptor FI (Figure 3b) was as expected.

UV−Vis Spectroscopy Study for the Modulation of Aβ Aggregates and Metal Chelation Confirmation. The retrieval of Cu^{2+} from Aβ1−40−Cu^{2+} aggregates was confirmed by UV−vis spectroscopy (Figure 4A, a−c) via formation of FI +Cu^{2+} complex.[85] The enhanced absorbance of Aβ (20 μM) + Cu^{2+} (20 μM) aggregates (1:1) was obtained at ∼264 nm which is 8 nm blue-shifted from the 272 nm of Aβ peptides due to the charge transfer mechanism (Figure 4A, a). The absorbance behavior of FI (10 and 20 μM) in the presence of Aβ−Cu^{2+} aggregates (1:1) was subsequently investigated after 24 h incubation. The wavelength of absorption of the closed-ring form of FI at 342 nm clearly vanished and a new absorption band appeared at 492 nm due to the formation of spirolactam ring opening of the xanthene moiety because of the formation of FI−Cu^{2+} complex by metal chelation. Further, a similar experiment performed with Aβ self-aggregates (without Cu^{2+}) in the presence of FI (20 μM), showed no response at 492 nm (Figure 4A, b). For the control studies, we performed an experiment between FI and free Cu^{2+} and the absorbance behavior of FI was investigated before and after the addition of Cu^{2+} (Figure 4A, c). The maximum absorption band at 342 nm was obtained for FI in its closed-ring form. Upon addition of Cu^{2+} (20 μM) into FI (20 μM) (1:1), a new absorption band appeared at 492 nm, accompanied by a change in the color from colorless to green which represents the open spirolactam ring form of the xanthene moiety. Such a huge ∼150 nm Cu^{2+}-induced absorption shift could be attributed to the high conjugation and planarity of the indole moiety of FI with the

DOI: 10.1021/acschemneuro.5b00205
ACS Chem. Neurosci. 2015, 6, 1880−1891

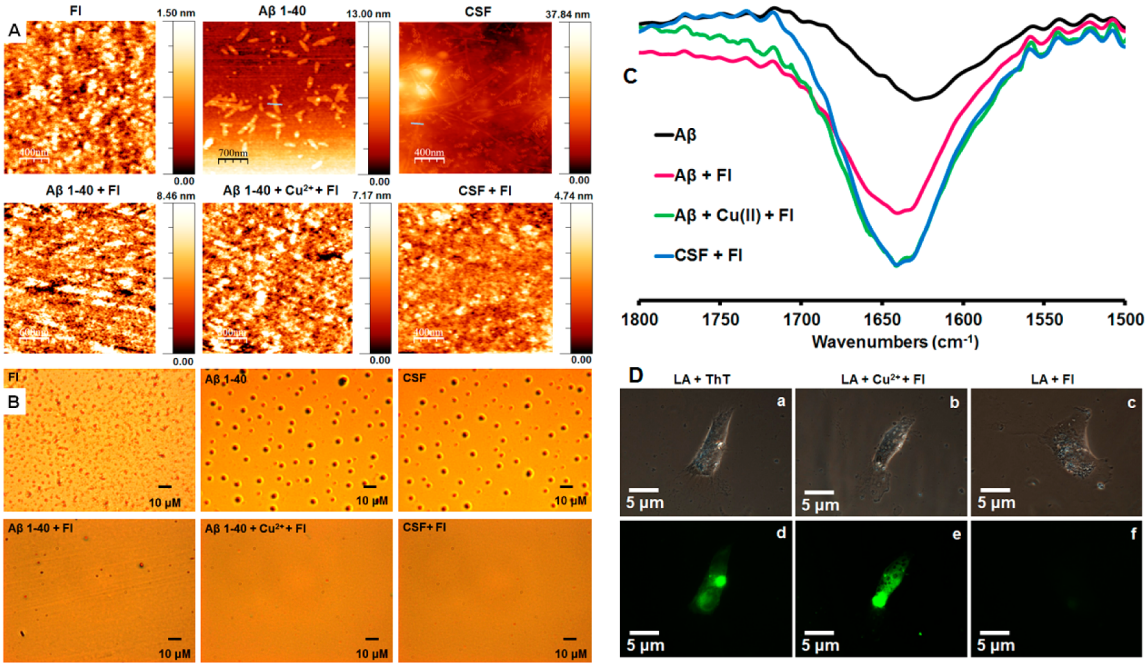

Figure 6. (A) AFM images of the morphologies of FI, Aβ1−40, and CSF fibrils (top left to right). Modulation or disaggregation effect of Aβ aggregates were observed by FI mixed Aβ1−40 in the absence and presence of Cu^{2+} and the modulation of CSF aggregates also observed in the presence of FI (bottom left to right) (samples incubated for ∼36 h). (B) Optical microscopy images of FI, β-sheet rich spherical images of Aβ1−40, and CSF Aβ aggregates (Top left to right). Modulation or disaggregation effects of Aβ aggregates were detected by FI mixed Aβ1−40 in the absence and presence of Cu^{2+} and FI mixed CSF (bottom left to right) (samples incubated for ∼36 h). (C) FT-IR spectra of β-sheet rich Aβ1−40 fibrils (black); pink, green, and blue lines indicate random coil structures of Aβ1−40−FI, Aβ1−40−Cu^{2+}−FI, and CSF−FI, respectively. (D) Disaggregation of β-amyloid LA was detected by fluorescence microscopy: (a−c) bright field images of LA−ThT, LA−Cu^{2+}−FI and LA−FI after 2 h incubation with U87 MG Human astrocytes cells. (d) Cells treated with β-sheet rich LA with ThT show fluorescence after 2 h incubation. (e) Fluorescence detected for the cells treated amyloid-β LA in the presence of Cu^{2+} with FI after incubation for 2 h. (f) No fluorescence was observed for amyloid-β LA with FI in the presence of Cu^{2+} after 2 h incubation (excitation at 460 nm).

binding sites which favors maximum negative charge distribution of the deprotonated receptor in the presence of Cu^{2+}.[57]

DLS Study to Determine the Size of Aggregated and Disaggregated or Modulated Form of Amyloid Aggregates. To determine the size of FI with aggregated Aβ peptides (Aβ1−40, CSF) and disaggregation or disruption of Aβ peptides (Aβ1−40, CSF) in the absence and presence of Cu^{2+} in aqueous solution, DLS measurements were performed on these samples. These experiments provided vital clues to arrive at a conclusion that FI could accelerate the disaggregation or disruption of Aβ peptides (Aβ 1−40, CSF) in aqueous solution as shown in Figure 4B, a−c. The control experiments confirmed that the hydrodynamic particle diameter of Aβ1−40 (530 ± 70 nm), Aβ1−40−Cu^{2+} (615 ± 100 nm), and Aβ peptides in CSF (712 ± 100 nm) were bigger in size as compared to the complex of FI−Aβ1−40 (295 ± 50 nm), FI−Aβ1−40−Cu^{2+} (295−340 nm), FI−CSF (295 ± 50 nm), and FI−CSF−Cu^{2+} (255−295 nm). Therefore, these results further validated that rapid and efficient disruption or disaggregation of Aβ peptide aggregates (Aβ1−40, CSF) could be achieved efficiently by the introduction of FI in the presence as well as the absence of Cu^{2+} (Figure 4B, a−c).

Preparation and Modulation of Lysozyme Aβ Aggregates. Large aggregated Aβ fibrils were obtained by heating lysozyme solution for 5 days (10 mg in 1 mL) at pH 2, 65 °C. The process of lysozyme fibrillation was confirmed by ThT binding assay where ThT is a commonly used to detect Aβ since it is reported to bind specifically to the characteristic β-sheet structure of Aβ fibrils (Figure 5). Morphologies of the formation of LA fibrils without Cu^{2+} and aggregated Aβ plaques with Cu^{2+} were detected by electronic microscopy images (SEM). For the modulation of LA fibrils and aggregated Aβ plaques, 20 μM of lysozyme aggregated fibrils (10 mM PBS, pH 7.4) were incubated without and with Cu^{2+} (20 μM) in the presence of FI (20 μM) at 37 °C for 2 days. These results demonstrated that FI treated lysozyme aggregated plaques and the Aβ fibrils were disaggregated or modulated completely due to the metal chelation and noncovalent interactions by FI.

Confirmation Studies of Aggregation and Disaggregation or Modulation of Aβ Aggregates. Morphological evidence for the disaggregation and modulation of Aβ1−40 fibrils and Cu^{2+}-Aβ1−40 aggregation in the presence of FI (Figure 6A) was obtained by AFM images. As demonstrated, Aβ1−40 aggregates showed well-defined Aβ fibrils after 36 h incubation at 37 °C. The existence of matured aggregated Aβ fibrils in CSF was also confirmed by AFM images (Figure 6A). Further, in the presence of FI, the Cu^{2+} induced Aβ1−40 aggregates were disaggregated completely due to the metal chelation by FI from the Aβ-Cu^{2+} complex.[86−89] The same experiment when performed using CSF Aβ fibrils in the presence of FI confirmed that the aggregated fibrils from the CSF were also disaggregated due to the metal chelation (Figure 6A). The AFM images obtained after the modulation experiments display completely different morphology unlike the Aβ fibrils (Aβ1−40 and CSF). Surprisingly the probe FI disaggregated and modulated the Aβ self-aggregated fibrils even

DOI: 10.1021/acschemneuro.5b00205
ACS Chem. Neurosci. 2015, 6, 1880−1891

in the absence of Cu^{2+} ions, due to the noncovalent interactions between FI and Aβ fibrils.[90−92]

The polarized optical microscopy (POM) images (Figure 6B) demonstrated that aggregated Aβ1−40 and CSF showed presence of spherical Aβ aggregates. These spherical aggregates of Aβ1−40, when incubated with FI for 36 h, in the absence as well as in the presence of Cu^{2+} and CSF mixed FI sample (Figure 6B), get disaggregated completely, confirming the ability of FI to convert Aβ aggregates into disaggregated forms.

The transformation of Aβ1−40 secondary structure was also examined by FT-IR spectroscopy (Figure 6C). The presence of a major band at 1629 ± 2 cm^{-1} indicates the parallel β-sheet conformation of Aβ1−40 aggregates (Figure 6C, black line).[93−97] The FT-IR spectra of FI mixed with β-sheet rich Aβ1−40 fibrils and with Aβ1−40−Cu^{2+} are shown as pink and green lines respectively (Figure 6C). The parallel β-sheet conformation of Aβ1−40 was transformed into the random coil conformation due to the structure modulation and metal chelation of Aβ1−40−Cu^{2+} with FI, as illustrated by a major band at 1644 ± 2 cm^{-1}. Similarly, CSF on incubation with FI for 36 h shows a major band at 1644 cm^{-1} confirming that FI converts β-sheet rich Aβ-aggregates in CSF into modulated random coil conformations (Figure 6C, blue line).

To establish whether FI can disaggregate and modulate the intracellular Aβ aggregates, we monitored the intracellular Aβ accumulation in U87 MG human astrocyte cells that had been loaded with Aβ LA overnight followed by treatment with Cu^{2+}/FI mixture. The cells treated with Aβ LA and stained with ThT shows bright green fluorescence in cell imaging experiments (Figures 6D, S6). As a control, the Aβ LA spread throughout the cells,[98,99] when treated without and with Cu^{2+} ions showed no green fluorescence of Aβ LA in the absence of ThT (Figure S7). The FI treated cells also did not show green fluorescence in intracellular Aβ LA without Cu^{2+} ions but in the presence of Cu^{2+} the Aβ LA showed green "turn-on" fluorescence due to the spirolactam ring opening of FI, proving that Cu^{2+} was chelated by FI and is in agreement with the in vitro experiments and the ThT assay results (Figures 6D, S6, and S7). This result also proves that disaggregation or disruption of Aβ fibrils was possible by abstracting Cu^{2+} ion from Aβ LA using FI probe in intracellular condition which is a major advancement for AD. Thus, FI has the exceptional ability to perform multiple tasks of metal chelation in aggregated Aβ LA in cellular environment and most importantly the disruption of β-sheets rich Aβ aggregates into disaggregated forms. Furthermore, FI also prevented their reaggregation into toxic forms which is one of the most crucial properties of a probe or a therapeutic agent to stop recurring of AD.

Cell Viability Assays. Endothelial cells were harvested from culture plate, and 25 000 cells were seeded per well in a 96-well plate. Twelve hours later, cells were treated with different concentrations of FI (0−200 μM) for 12 h (Figure S8). The dose dependent toxicity of FI was observed at various time points by the standard MTT assay. After 12 h exposure of FI (100 μM) to cells, less than 5% inhibition of cell growth was observed. However, at 200 μM concentration, the cells experienced ∼15% toxicity. This observation led to utilization of 100 μM FI for the endothelial monolayer permeability assay.

Endothelial Monolayer Permeability Assays. FI mediated disaggregation of Aβ fibrils were also studied in a cellular environment. These fibrils are formed and accumulated within brain neuronal cells during AD and the brain cells remain protected by the blood-brain barrier (BBB). To act against the Aβ fibrils, this FI had to cross the BBB. Therefore, to examine the BBB crossing ability of FI, a monolayer of human endothelial cells, EA.hy926, was used as an in vitro BBB model.[100,101] Prior to the BBB permeability assay, cytotoxicity of FI to endothelial cells was assessed (Figure S8) and a noncytotoxic concentration of 100 μM of FI was used to check in vitro BBB crossing ability as described in the Methods. The post experimental analysis revealed that, during the first hour, the obtained level of FI in the lower chamber was ∼65% ± 1. Later, the level of FI increased with time and reached maximum ∼94% ± 2 at 4 and 6 h (Figure 7). During this period, the cellular morphology remained unchanged and no visible cellular damage or death was observed (inset, Figure 7). Thus, the observation of in vitro endothelial monolayer permeability model directly indicated that FI can across BBB.

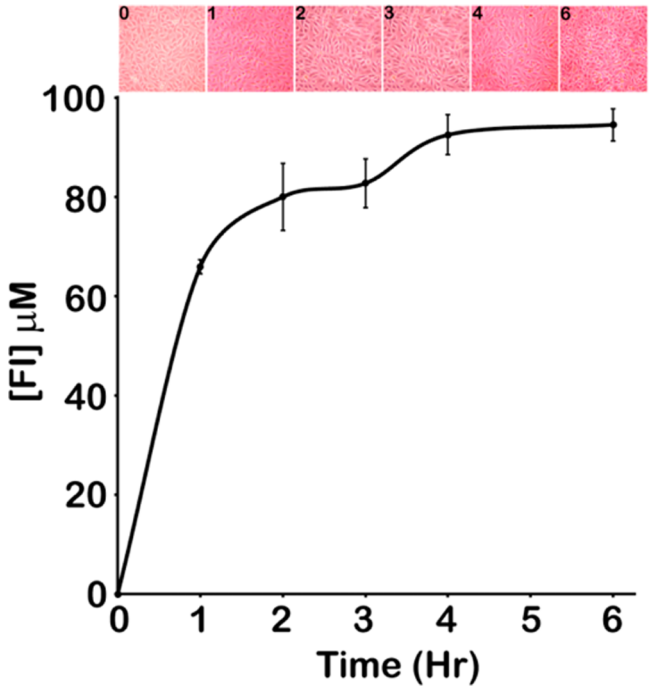

Figure 7. FI can cross the endothelial monolayer barrier: Endothelial cells were plated on 3 μM polycarbonate transwell membrane in DMEM supplemented with 10% FBS and allowed to grow to confluence. FI (100 μM) solution prepared in complete media was added in the upper chamber, and after every 1 h media (∼1 mL) was collected from the lower chamber and level of FI was quantified by fluorescence spectroscopy (excitation at 342 nm). The morphology of the endothelial monolayer during the experiment was observed with an inverted microscope TS100 attached to high resolution camera and given in the inset.

CONCLUSION

In summary, the disruption, modulation, and elimination of Aβ fibrillar plaques along with metal ions such as Cu(II), Fe(II, III), and Zn(II) are very vital for the prevention of several neurological disorders. Development of metal chelating probes that can selectively bind metals lying deep within the Aβ plaques, CSF, or larger systems such as Aβ LA and competitive cellular environment have never been attempted previously. This multiple approach would have immense impact on the etiology of AD and help in developing newer AD therapeutic strategies. The simple indole-3-carboxaldehyde fluorescein

DOI: 10.1021/acschemneuro.5b00205
ACS Chem. Neurosci. 2015, 6, 1880−1891

hydrazone (FI) probe was nontoxic up to a concentration of 100 μM and was observed to have endothelial monolayer permeability, confirming its ability to cross the blood-brain barrier. FI performs multiple tasks of disaggregating and modulating the Aβ aggregates in the absence and presence of Cu^{2+} in Aβ fibrils, CSF, and Aβ LA in U87 MG human astrocyte cells and prevents them from aggregating again. Most importantly, FI effectively modulated the assembly of metal-free Aβ aggregates also by noncovalent interactions over and above its exceptional ability to bind Cu^{2+} and disrupt the metal-induced Aβ aggregates. This metal chelation resulted in the "turn-on" fluorescence of FI probe via spirolactam ring opening. Although intracellular disaggregation of Aβ fibrils in presence as well as absence of cupric ions is demonstrated in multiple environments by FI, more research is required to improve our understanding on the role of copper and other metals in the pathogenesis of AD and neurologic disorders which would help to envision and design better therapeutic molecules to influence the amyloidogenesis.

METHODS

Materials. All the reagents and chemicals were purchased from Aldrich Chemicals, Merck, or Ranbaxy (India) and were used as received. Milli-Q water and HPLC grade solvents were used in all the experiments. Solvents were degassed using three freeze−thaw cycles or flushed with nitrogen for at least 1 h prior to use when necessary. β-Amyloid (1−40), human, was purchased from G L Biochem Ltd., Shanghai, China. The cerebrospinal fluid (CSF) samples were gifted by Guwahati Neurological Research Center and Hospital, Guwahati, India and were obtained as part of routine care from patients. Nonetheless, information on explaining the purpose of this study was specified at the time of sample collection adhering to the bioethics policy of the hospital.

Instrumentation. UV−vis absorption spectra were recorded on a PerkinElmer Lambda-25 spectrometer. Fluorescence spectra were carried out on a Varian Cary Eclipse spectrometer. A 10 mm × 10 mm quartz cuvette was used for solution spectra, and emission was collected at 90° relative to the excitation beam. A Leica polarizable optical microscope was used to image the aggregation and disruption studies. A Nikon Eclipse 80i microscope was used to study the fluorescent images. FT-IR spectra were recorded on a PerkinElmer spectrometer with samples prepared as KBr pellets. A fresh glass slide was used for every experiment. Deionized water was obtained from a Milli-Q system (Millipore). SEM images were investigated by scanning electron microscopy (SEM) on a LEO 1430vp instrument operated at 8−10 kV. Atomic force microscopy (AFM) was recorded on an Agilent instrument, model 5500 series, with noncontact mode. DLS were measured using a Zetasizer Nano series Nano-ZS90 instrument. The POM images were obtained on a Leica DM 2500P microscope.

Preparation of FI Stock Solution. The ligand FI stock solution was prepared at the concentration of 1.0×10^{-3} mL^{-1} in 10 mL DMSO. This stock solution was diluted to desired concentration for each titration in 3 mL cuvette.

Preparation of HEPES Buffer Solutions. All the UV−visible and fluorescence titrations were performed in 10 mM HEPES buffer and pH maintained at 7.4 by using 4 M NaOH or 5 M HCl solution.

TFA/HFIP Treatment of Aβ (1−40). Aβ (1−40) was disaggregated using trifluoroacetic acid/1,1,1,3,3,3-hexafluuor-2-propanol (TFA/HFIP) by an established method (references mentioned in the Supporting Information). The amount of 0.5 mg of Aβ (1−40) was added to a 2.5 mL eppendorf tube and dissolved in TFA to obtain a homogeneous solution free of aggregates. TFA was then evaporated using argon gas. Any leftover TFA was further removed by adding HFIP followed by evaporation using an argon gas flow to obtain a film like material. This process was repeated twice. To the eppendorf tube, 2.5 mL of HEPES (10 mM, pH 7.4) was added followed by sonication and vortexing to obtain a final concentration of 4.6×10^{-4} M. Fibril formation was monitored using a ThT binding assay.

ThT Binding Assay. ThT fluorescence was measured with fluorescence excitation at 440 nm and emission detection at 487 nm. The 20 μM concentration of Aβ1−40 and ThT (20 μM) was used in all the experiments. The concentration of 20 μM Cu^{2+} and FI solution were used where needed for the experiments. The sample was prepared in a final volume of 600 μL in HEPES (10 mM, pH 7.4) and kept for incubation at 37 °C in water bath.

Tyrosine Fluorescence Spectroscopy. The 20 μM concentration of Aβ1−40 and 10 or 20 μM Cu^{2+} and FI solution were used where needed for the experiments. The sample was prepared in the final volume of 600 μL in HEPES (10 mM, pH 7.4) and dequenching sample kept at incubation for 48 h at 37 °C in water bath. Fluorescence measurements were performed in a 1 mL quartz fluorescence cuvette with excitation at 274 nm (slit 10 nm) and emission detection at 305 nm (slit 10 nm) in 10 mM HEPES buffer (pH 7.4). Tyrosine fluorescence spectroscopy was used to monitor the binding of Cu^{2+} to Aβ1−40. It is well established that Cu^{2+} binds to Aβ1−40 and quenches the tyrosine fluorescence.

Confirmation of CSF Aβ Aggregates Using ThT Binding Assay. The existence of Aβ fibrils in CSF was confirmed by the addition of CSF sample up to 100 μL solution (20, 50, and 100 μL) into ThT (20 μM) solution (pH 7.4 in HEPES) to observe a enhancement in the fluorescence intensity of ThT at 487 nm validating strongly the existence of aggregated Aβ fibrils in the CSF sample.

Sample Preparation for Atomic Force Microscopy (AFM) Images. Morphologies of Aβ1−40 and CSF aggregates were studied by AFM. Aβ1−40 peptides (20 μM) in buffer solution (10 mM HEPES, pH 7.4) were incubated with and without Cu^{2+} (20 μM) as well as in the presence and absence of FI (20 μM) at 37 °C for 2 days. Further, all the solutions were separately diluted by 10 times, and then from the diluted solutions 5 μL of the sample was mounted onto the freshly cleaned glass slide for 12 h incubation, gently rinsed with deionized water, and dried at room temperature overnight and then AFM was recorded on an Agilent instrument, model 5500 series, with noncontact mode.

FTIR Sample Preparation. Aβ1−40 peptides (20 μM) in buffer solution (10 mM HEPES, pH 7.4) were incubated with or without Cu^{2+} (20 μM) and in presence or absence of FI (20 μM) at 37 °C for 2 days. A volume of 10 μL of the sample was mounted onto the freshly cleaned glass slide for 12 h incubation, gently rinsed with deionized water, and dried at room temperature overnight, and then FT-IR spectra recorded on a PerkinElmer spectrometer with samples prepared as KBr pellets.

Polarized Optical Microscopy Study. Images of Aβ1−40 and CSF aggregates were detected by optical microscopy. Aβ1−40 peptides (20 μM) in buffer solution (10 mM HEPES, pH 7.4) were incubated with and without Cu^{2+} (20 μM) as well as in the presence and absence of FI (20 μM) at 37 °C for 2 days. Samples were prepared by spreading 30 μL of each solution on a glass slide and then incubating at room temperature for 48 h. Then images were observed for all the incubated samples under a Leica DM 2500P microscope.

Preparation of Lysozyme Fibrils. The amyloid fibrils were obtained by heating lysozyme solution (10 mg in 1 mL) in pH 2 at 65 °C for 5 days. The process of lysozyme fibrillation was confirmed by ThT binding assay, where ThT is commonly used as an amyloid detector as it is reported to bind specifically to the characteristic β-sheet structure of amyloid fibrils.

SEM Images of Lysozyme Aggregated (LA) Fibrils and Amyloid Plaques. Morphologies of the formation of LA fibrils without Cu^{2+} and aggregated amyloid plaques with Cu^{2+} were detected by SEM. For the modulation of LA fibrils and aggregated amyloid plaques, 20 μM lysozyme aggregated fibrils (10 mM PBS, pH 7.4) was incubated without and with Cu^{2+} (20 μM) in the presence of FI (20 μM) at 37 °C for 2 days. Result show that FI treated lysozyme aggregated plaques and fibrils were disaggregated or disturbed due to the metal chelation and noncovalent interactions by FI.

DOI: 10.1021/acschemneuro.5b00205
ACS Chem. Neurosci. 2015, 6, 1880−1891

Cell Culture and Treatment. U87-MG cell line was procured from NCCS, Pune. Cells were cultured in Dulbecco's modified Eagle's media (DMEM) (Sigma, St. Louis, MO), supplemented with 10% fetal bovine serum (FBS) and 1% penicillin−streptomycin antibiotic (100 units/mL penicillin and 100 μg/mL streptomycin sulfate) and grown at 37 °C in a humidified 5% CO_2 incubator. On the day of the experiment, cells were washed with PBS and loaded with β-amyloid lysozyme aggregate (LA) (1 mg in 1 mL). All wells were washed with PBS at least two times and treated with Cu^{2+} (50 μM) for 1 h. Cells were washed again with PBS three times and treated with FI (100 μM and 400 μM) for 1−2 h. To detect LA inside the cells, all samples were treated with ThT (100 μg/mL) for 1 h. Cells loaded with lysozyme solution (1 mg in 1 mL) serves as a negative control.

Fluorescence Microscopic Detection and Disaggregation of Lysozyme Aggregated (LA) Fibrils and Amyloid Plaques. Each coverslip containing cells was fixed in 4% paraformaldehyde at 37 °C for 30 min, mounted, and observed under fluorescence microscopy. Cells loaded with β-amyloid LA gave intense fluorescence signal at 350 and 485 nm when cells were treated with FI/Cu^{2+} mixture from 1 to 2 h. The fluorescence intensity increased significantly over time of exposure of the probe to copper ions inside the cells containing lysozyme fibrils.

Cell Viability Assays. DMEM-high glucose (D5648-sigma), FBS (RM10432-Himedia), Thiazolyl Blue Tetrazolium Bromide (M2128-Sigma), DMSO (61857105001730-Merck), and Whatman filter paper 42 (1442-125, GE Healthcare). Human endothelial cells (EA.hy926) were purchased from ATCC and cultured in DMEM high glucose media containing 10% FBS.

Endothelial cells were harvested from culture plate, and 25 000 cells were seeded per well in 96-well plates. Twelve hours later, cells were treated with different concentration of FI (0 to 200 μM) for 12 h. Cell viability was assessed by following the standard MTT assay protocol. The formed formazone crystals were measured at 570 nm by using the Spectromax M2e microtiter plate reader.

Endothelial Monolayer Permeability Assays. The immortalized endothelial cells (EA.hy926) were plated on 3 μm polycarbonate transwell membranes in DMEM supplemented with 10% FBS. After reaching confluence, the media in the upper chamber was removed and the complete media containing FI (100 μM) was added to the upper well. The media was collected at different time point intervals (1−6 h) to quantify the FI compound level by using fluorescence spectroscopy and simultaneously images were collected (1−6 h) by using a Nikon TS100 microscope.

■ ASSOCIATED CONTENT

Supporting Information

The Supporting Information is available free of charge on the ACS Publications website at DOI: 10.1021/acschemneuro.5b00205.

Details of methods used in performing various imaging; experiments details (PDF)

■ AUTHOR INFORMATION

Corresponding Authors

*E-mail: vtrivedi@iitg.ernet.in (V.T.).
*E-mail: pki@iitg.ernet.in (P.K.I.).

Funding

Financial support from Department of Science and Technology (DST), India (No. DST/SERB/EMR/2014/000034, No. DST/TSG/PT/2009/11 & 23), DST−Max Planck Society, Germany (IGSTC/MPG/PG(PKI)/2011A/48), and Department of Information Technology, DeitY project No. 5(9)/2012-NANO (Vol. II) are acknowledged.

Notes

The authors declare no competing financial interest.

■ REFERENCES

(1) Holtzman, D. M., Morris, J. C., and Goate, A. M. (2011) Alzheimer's Disease: The challenge of the second century. *Sci. Transl. Med. 3*, 77.

(2) Thies, W., and Bleiler, L. (2013) Alzheimer's disease facts and figures. *Alzheimer's Dementia 9*, 208.

(3) Viles, J. H. (2012) Metal ions and amyloid fiber formation in neurodegenerative diseases. Copper, zinc and iron in Alzheimer's, Parkinson's and Prion diseases. *Coord. Chem. Rev. 256*, 2271.

(4) Valensin, D., Gabbiani, C., and Messori, L. (2012) Metal compounds as inhibitors of β -amyloid aggregation. Perspectives for an innovative metallotherapeutics on Alzheimer's disease. *Coord. Chem. Rev. 256*, 2357.

(5) Wang, Y.-J., Zhou, H.-D., and Zhou, X.-F. (2006) Clearance of amyloid-beta in Alzheimer's disease: progress, problems and perspectives. *Drug Discovery Today 11*, 931.

(6) Jakob-Roetne, R., and Jacobsen, H. (2009) Alzheimer's disease: From pathology to therapeutic approaches. *Angew. Chem., Int. Ed. 48*, 3030.

(7) Buxbaum, J. N., and Linke, R. P. (2012) A molecular history of the amyloidoses. *J. Mol. Biol. 421*, 142.

(8) Rauk, A. (2009) The chemistry of Alzheimer's disease. *Chem. Soc. Rev. 38*, 2698.

(9) Pithadia, A. S., and Lim, M. H. (2012) Metal-associated amyloid-β species in Alzheimer's disease. *Curr. Opin. Chem. Biol. 16*, 67.

(10) Faller, P., and Hureau, C. (2009) Bioinorganic chemistry of copper and zinc ions coordinated to amyloid-β peptide. *Dalton Trans.*, 1080.

(11) Drew, S. C., and Barnham, K. J. (2011) The heterogeneous nature of Cu^{2+} interactions with Alzheimer's amyloid-β peptide. *Acc. Chem. Res. 44*, 1146.

(12) Scott, L. E., and Orvig, C. (2009) Medicinal inorganic chemistry approaches to passivation and removal of aberrant metal ions in disease. *Chem. Rev. 109*, 4885.

(13) Savelieff, M. G., Lee, S., Liu, Y., and Lim, M. H. (2013) Untangling amyloid-β, tau, and metals in Alzheimer's disease. *ACS Chem. Biol. 8*, 856.

(14) Hureau, C. (2012) Coordination of redox active metal ions to the amyloid precursor protein and to amyloid-β peptides involved in Alzheimer disease. Part 1: An overview. *Coord. Chem. Rev. 256*, 2164.

(15) Hureau, C., and Dorlet, P. (2012) Coordination of redox active metal ions to the amyloid precursor protein and to amyloid-β peptides involved in Alzheimer disease. Part 2: Dependence of Cu(II) binding sites with Aβ sequences. *Coord. Chem. Rev. 256*, 2175.

(16) Smith, D. G., Cappai, R., and Barnham, K. J. (2007) The redox chemistry of the Alzheimer's disease amyloid β peptide. *Biochim. Biophys. Acta, Biomembr. 1768*, 1976.

(17) Roychaudhuri, R., Yang, M., Hoshi, M. M., and Teplow, D. B. (2009) Amyloid-β protein assembly and Alzheimer disease. *J. Biol. Chem. 284*, 4749.

(18) Zhu, X., Su, B., Wang, X., Smith, M. A., and Perry, G. (2007) Causes of oxidative stress in Alzheimer disease. *Cell. Mol. Life Sci. 64*, 2202.

(19) Kozlowski, H., Luczkowski, M., Remelli, M., and Valensin, D. (2012) Copper, zinc and iron in neurodegenerative diseases (Alzheimer's, Parkinson's and Prion diseases). *Coord. Chem. Rev. 256*, 2129.

(20) Duce, J. A., and Bush, A. I. (2010) Biological metals and Alzheimer's disease: Implications for therapeutics and diagnostics. *Prog. Neurobiol. 92*, 1.

(21) Alies, B., Pradines, V., Llorens-Alliot, I., Sayen, S., Guillon, E., Hureau, C., and Faller, P. (2011) Zinc(II) modulates specifically amyloid formation and structure in model peptides. *JBIC, J. Biol. Inorg. Chem. 16*, 333.

(22) Maret, W. (2012) New perspectives of zinc coordination environments in proteins. *J. Inorg. Biochem. 111*, 110.

(23) Savelieff, M. G., DeToma, A. S., Derrick, S. S., and Lim, M. H. (2014) The ongoing search for small molecules to study metal-

DOI: 10.1021/acschemneuro.5b00205
ACS Chem. Neurosci. 2015, 6, 1880−1891

associated amyloid-β species in Alzheimer's disease. *Acc. Chem. Res. 47*, 2475.
(24) Nguyen, M., Robert, A., Sournia-Saquet, A., Vendier, L., and Meunier, B. (2014) Characterization of new specific copper chelators as potential drugs for the treatment of Alzheimer's disease. *Chem. - Eur. J. 20*, 6771.
(25) Savelieff, M. G., Lee, S., Liu, Y., and Lim, M. H. (2013) Untangling amyloid-β, tau, and metals in Alzheimer's disease. *ACS Chem. Biol. 8*, 856.
(26) Pithadia, A. S., and Lim, M. H. (2012) Metal-associated amyloid-β species in Alzheimer's disease. *Curr. Opin. Chem. Biol. 16*, 67.
(27) Khan, A., Ashcroft, A. E., Korchazhkina, O. V., and Exley, C. (2004) Metal-mediated formation of fibrillar ABri amyloid. *J. Inorg. Biochem. 98*, 2006.
(28) McLachlan, D. R. C., Dalton, A. J., Kruck, T. P., Bell, M. Y., Smith, W. L., Kalow, W., and Andrews, D. F. (1991) Intramuscular desferrioxamine in patients with Alzheimer's disease. *Lancet 337*, 1304.
(29) Cherny, R. A., Legg, J. T., McLean, C. A., Fairlie, D. P., Huang, X., Atwood, C. S., Beyreuther, K., Tanzi, R. E., Masters, C. L., and Bush, A. I. (1999) Aqueous dissolution of Alzheimer's disease Aβ amyloid deposits by biometal depletion. *J. Biol. Chem. 274*, 23223.
(30) Franz, K. J. (2013) Clawing back: Broadening the notion of metal chelators in medicine. *Curr. Opin. Chem. Biol. 17*, 143.
(31) Ritchie, C. W., Bush, A. I., Mackinnon, A., Macfarlane, S., Mastwyk, M., MacGregor, L., Kiers, L., Cherny, R., Li, Q. X., Tammer, A., Carrington, D., Mavros, C., Volitakis, I., Xilinas, M., Ames, D., Davis, S., Beyreuther, K., Tanzi, R. E., and Masters, C. L. (2003) Metal-protein attenuation with iodochlorhydroxyquin (clioquinol) targeting Abeta amyloid deposition and toxicity in Alzheimer disease: A pilot phase 2 clinical trial. *Arch. Neurol. 60*, 1685.
(32) Lannfelt, L., Blennow, K., Zetterberg, H., Batsman, S., Ames, D., Harrison, J., Masters, C. L., Targum, S., Bush, A. I., Murdoch, R., Wilson, J., and Ritchie, C. W. (2008) Safety, efficacy, and biomarker findings of PBT2 in targeting Aβ as a modifying therapy for Alzheimer's disease: a phase IIa, double-blind, randomized, placebo-controlled trial. *Lancet Neurol. 7*, 779.
(33) Cherny, R. A., Atwood, C. S., Xilinas, M. E., Gray, D. N., Jones, W. D., McLean, C. A., Barnham, K. J., Volitakis, I., Fraser, F. W., Kim, Y.-S., Huang, X., Goldstein, L. E., Moir, R. D., Lim, J. T., Beyreuther, K., Zheng, H., Tanzi, R. E., Masters, C. L., and Bush, A. I. (2001) Treatment with a copper-zinc chelator markedly and rapidly inhibits beta-amyloid accumulation in Alzheimer's disease transgenic mice. *Neuron 30*, 665.
(34) Crouch, P. J., Tew, D. J., Du, T., Nguyen, D. N., Caragounis, A., Filiz, G., Blake, R. E., Trounce, I. A., Soon, C. P. W., Laughton, K., Perez, K. A., Li, Q.-X., Cherny, R. A., Masters, C. L., Barnham, K. J., and White, A. R. (2009) Restored degradation of the Alzheimer's amyloid-β peptide by targeting amyloid formation. *J. Neurochem. 108*, 1198.
(35) Faux, N. G., Ritchie, C. W., Gunn, A., Rembach, A., Tsatsanis, A., Bedo, J., Harrison, J., Lannfelt, L., Blennow, K., Zetterberg, H., Ingelsson, M., Masters, C. L., Tanzi, R. E., Cummings, J. L., Herd, C. M., and Bush, A. I. (2010) PBT2 rapidly improves cognition in Alzheimer's Disease: additional phase II analyses. *J. Alzheimer's Dis. 20*, 509.
(36) DeToma, A. S., Salamekh, S., Ramamoorthy, A., and Lim, M. H. (2012) Misfolded proteins in Alzheimer's disease and type II diabetes. *Chem. Soc. Rev. 41*, 608.
(37) Telpoukhovskaia, M. A., and Orvig, C. (2013) Werner coordination chemistry and neurodegeneration. *Chem. Soc. Rev. 42*, 1836.
(38) Pithadia, A. S., Kochi, A., Soper, M. T., Beck, M. W., Liu, Y., Lee, S., DeToma, A. S., Ruotolo, B. T., and Lim, M. H. (2012) Reactivity of diphenylpropynone derivatives toward metal-associated amyloid-β Species. *Inorg. Chem. 51*, 12959.
(39) Braymer, J. J., Choi, J.-S., DeToma, A. S., Wang, C., Nam, K., Kampf, J. W., Ramamoorthy, A., and Lim, M. H. (2011) Development of bifunctional stilbene derivatives for targeting and modulating metal-amyloid-β species. *Inorg. Chem. 50*, 10724.
(40) Liu, Y., Kochi, A., Pithadia, A. S., Lee, S., Nam, Y., Beck, M. W., He, X., Lee, D., and Lim, M. H. (2013) Tuning reactivity of diphenylpropynone derivatives with metal-associated amyloid-β species via structural modifications. *Inorg. Chem. 52*, 8121.
(41) Porter, M. R., Kochi, A., Karty, J. A., Lim, M. H., and Zaleski, J. M. (2015) Chelation-induced diradical formation as an approach to modulation of the amyloid-β aggregation pathway. *Chem. Sci. 6*, 1018.
(42) Rodríguez-Rodríguez, C., Telpoukhovskaia, M., and Orvig, C. (2012) The art of building multifunctional metal-binding agents from basic molecular scaffolds for the potential application in neuro-degenerative diseases. *Coord. Chem. Rev. 256*, 2308.
(43) DeToma, A. S., Salamekh, S., Ramamoorthy, A., and Lim, M. H. (2012) Misfolded proteins in Alzheimer's disease and type II diabetes. *Chem. Soc. Rev. 41*, 608.
(44) Braymer, J. J., DeToma, A. S., Choi, J.-S., Ko, K. S., and Lim, M. H. (2011) Recent development of bifunctional small molecules to study metal amyloid-β species in Alzheimer's disease. *Int. J. Alzheimer's Dis. 2011*, 623051.
(45) Scott, L. E., Telpoukhovskaia, M., Rodrıguez-Rodrıguez, C., Merkel, M., Bowen, M. L., Page, B. D. G., Green, D. E., Storr, T., Thomas, F., Allen, D. D., Lockman, P. R., Patrick, B. O., Adam, M. J., and Orvig, C. (2011) N-Aryl-substituted 3-(b-D-glucopyranosyloxy)-2-methyl-4(1H)-pyridinones as agents for Alzheimer's therapy. *Chem. Sci. 2*, 642.
(46) Alies, B., Sasaki, I., Proux, O., Sayen, S., Guillon, E., Faller, P., and Hureau, C. (2013) Zn impacts Cu coordination to amyloid-β, the Alzheimer's peptide, but not the ROS production and the associated cell toxicity. *Chem. Commun. 49*, 1214.
(47) Pramanik, D., and Dey, S. G. (2011) Active site environment of heme-bound amyloid β peptide associated with Alzheimer's disease. *J. Am. Chem. Soc. 133*, 81.
(48) Guilloreau, L., Combalbert, S., Sournia-Saquet, A., Mazarguil, H., and Faller, P. (2007) Redox chemistry of copper-amyloid-β: The generation of hydroxyl radical in the presence of ascorbate is linked to redox-potentials and aggregation state. *ChemBioChem 8*, 1317.
(49) Curtain, C. C., Ali, F., Volitakis, I., Cherny, R. A., Norton, R. S., Beyreuther, K., Barrow, C. J., Masters, C. L., Bush, A. I., and Barnham, K. J. (2001) Alzheimer's disease amyloid-β binds copper and zinc to generate an allosterically ordered membrane-penetrating structure containing superoxide dismutase-like subunits. *J. Biol. Chem. 276*, 20466.
(50) Smith, D. P., Smith, D. G., Curtain, C. C., Boas, J. F., Pilbrow, J. R., Ciccotosto, G. D., Lau, T.-L., Tew, D. J., Perez, K., Wade, J. D., Bush, A. I., Drew, S. C., Separovic, F., Masters, C. L., Cappai, R., and Barnham, K. J. (2006) Copper-mediated amyloid-β toxicity is associated with an intermolecular histidine bridge. *J. Biol. Chem. 281*, 15145.
(51) Smith, D. G., Cappai, R., and Barnham, K. J. (2007) The redox chemistry of the Alzheimer's disease amyloid β peptide. *Biochim. Biophys. Acta, Biomembr. 1768*, 1976.
(52) Galeazzi, L., Ronchi, P., Franceschi, C., and Giunta, S. (1999) In vitro peroxidase oxidation induces stable dimers of β-amyloid (1−42) through dityrosine bridge formation. *Amyloid 6*, 7.
(53) Giunta, S., Ronchi, P., Valli, B., Franceschi, C., and Galeazzi, L. (2000) Transformation of beta-amyloid (Aβ) (1−42) tyrosine to L-Dopa as the result of in vitro hydroxyl radical attack. *Amyloid 7*, 189.
(54) Rolinski, O. J., Amaro, M., and Birch, D. J. S. (2010) Early detection of amyloid aggregation using intrinsic fluorescence. *Biosens. Bioelectron. 25*, 2249.
(55) Amaro, M., Birch, D. J. S., and Rolinski, O. J. (2011) Beta-amyloid oligomerisation monitored by intrinsic tyrosine fluorescence. *Phys. Chem. Chem. Phys. 13*, 6434.
(56) Jensen, M., Canning, A., Chiha, S., Bouquerel, P., Pedersen, J. T., Østergaard, J., Cuvillier, O., Sasaki, I., Hureau, C., and Faller, P. (2012) Inhibition of Cu-amyloid-β by using bifunctional peptides with β-sheet breaker and chelator moieties. *Chem. - Eur. J. 18*, 4836.

DOI: 10.1021/acschemneuro.5b00205
ACS Chem. Neurosci. 2015, 6, 1880−1891

(57) Muthuraj, B., Deshmukh, R., Trivedi, V., and Iyer, P. K. (2014) Highly selective probe detects cu^{2+} and endogenous no gas in living cell. *ACS Appl. Mater. Interfaces 6*, 6562.
(58) Maiti, N. C., Jiang, D., Wain, A. J., Patel, S., Dinh, K. L., and Zhou, F. (2008) Mechanistic Studies of Cu (II) Binding to Amyloid-peptides and the fluorescence and redox behaviors of the resulting complexes. *J. Phys. Chem. B 112*, 8406.
(59) Karr, J. W., Akintoye, H., Kaupp, L. J., and Szalai, V. A. (2005) N-Terminal deletions modify the Cu^{2+} binding site in amyloid-β. *Biochemistry 44*, 5478.
(60) Syme, C. D., Nadal, R. C., Rigby, S. E. J., and Viles, J. H. (2004) Copper binding to the amyloid-β (Aβ) peptide associated with Alzheimer's Disease. *J. Biol. Chem. 279*, 18169.
(61) Ma, Q. F., Hu, J., Wu, W. H., Liu, H. D., Du, J. T., Fu, Y., Wu, Y. W., Lei, P., Zhao, Y. F., and Li, Y. M. (2006) Characterization of copper binding to the peptide amyloid-β (1−16) associated with Alzheimer's Disease. *Biopolymers 83*, 20.
(62) Atwood, C. S., Perry, G., Zeng, H., Kato, Y., Jones, W. D., Ling, K. Q., Huang, X., Moir, R. D., Wang, D., Sayre, L. M., Smith, M. A., Chen, S. G., and Bush, A. I. (2004) Copper mediates dityrosine cross-linking of Alzheimer's amyloid-β. *Biochemistry 43*, 560.
(63) Wu, W., Lei, P., Liu, Q., Hu, J., Gunn, A. P., Chen, M., Rui, Y., Su, X., Xie, Z., Zhao, Y., Bush, A. I., and Li, Y. (2008) Sequestration of copper from β-amyloid promotes selective lysis by cyclen-hybrid cleavage agents. *J. Biol. Chem. 283*, 31657.
(64) Yu, M., Ryan, T. M., Ellis, S., Bush, A. I., Triccas, J. A., Rutledge, P. J., and Todd, M. H. (2014) Neuroprotective peptide−macrocycle conjugates reveal complex structure−activity relationships in their interactions with amyloid β. *Metallomics 6*, 1931.
(65) Alies, B., Renaglia, E., Rózga, M., Bal, W., Faller, P., and Hureau, C. (2013) Cu(II) affinity for the Alzheimer's peptide: Tyrosine fluorescence studies revisited. *Anal. Chem. 85*, 1501.
(66) Lincoln, K. M., Gonzalez, P., Richardson, T. E., Julovich, D. A., Saunders, R., Simpkins, J. W., and Green, K. N. (2013) A potent antioxidant small molecule aimed at targeting metal-based oxidative stress in neurodegenerative disorders. *Chem. Commun. 49*, 2712.
(67) Scott, L. E., Page, B. D. G., Patrick, B. O., and Orvig, C. (2008) Altering pyridinone N-substituents to optimize activity as potential prodrugs for Alzheimer's disease. *Dalton Trans.*, 6364.
(68) Chen, W., Wang, X., He, Y., Zhang, C., Wu, Z., Liao, K., Wang, J., and Guo, Z. (2009) Effects of Cyclen and Cyclam on Zinc(II)- and Copper(II)-Induced Amyloid β-Peptide Aggregation and Neurotoxicity. *Inorg. Chem. 48*, 5801.
(69) Faller, P., Hureau, C., Dorlet, P., Hellwig, P., Coppel, Y., Collin, F., and Alies, B. (2012) Methods and techniques to study the bioinorganic chemistry of metal-peptide complexes linked to neurodegenerative diseases. *Coord. Chem. Rev. 256*, 2381.
(70) Zhu, L., Han, Y., He, C., Huang, X., and Wang, Y. (2014) Disaggregation Ability of Different Chelating Molecules on Copper Ion-Triggered Amyloid Fibers. *J. Phys. Chem. B 118*, 9298.
(71) Ma, Q., Wei, G., and Yang, X. (2013) Influence of Au nanoparticles on the aggregation of amyloid-β-(25−35) peptides. *Nanoscale 5*, 10397.
(72) Ban, T., Hamada, D., Hasegawa, K., Naiki, H., and Goto, Y. (2003) Direct observation of amyloid fibril growth monitored by Thioflavin T fluorescence. *J. Biol. Chem. 278*, 16462.
(73) Anand, U., and Mukherjee, M. (2013) Exploring the self-assembly of a short aromatic aβ(16−24) peptide. *Langmuir 29*, 2713.
(74) Pedersen, J. T., Østergaard, J., Rozlosnik, N., Gammelgaard, B., and Heegaard, N. H. (2011) Cu(II) mediates kinetically distinct, non-amyloidogenic aggregation of amyloid-β peptides. *J. Biol. Chem. 286*, 26952.
(75) Pedersen, J. T., Teilum, K., Heegaard, N. H., Østergaard, J., Adolph, H. W., and Hemmingsen, L. (2011) Rapid formation of a preoligomeric peptide−metal−peptide complex following copper(ii) binding to amyloid β peptides. *Angew. Chem., Int. Ed. 50*, 2532.
(76) Muthuraj, B., Hussain, S., and Iyer, P. K. (2013) A rapid and sensitive detection of ferritin at a nanomolar level and disruption of amyloid β fibrils using fluorescent conjugated polymer. *Polym. Chem. 4*, 5096.
(77) Liu, L., Zhang, L., Mao, X., Niu, L., Yang, Y., and Wang, C. (2009) Chaperon-mediated single molecular approach toward modulating aβ peptide aggregation. *Nano Lett. 9*, 4066.
(78) Liu, L., Zhang, L., Niu, L., Xu, M., Mao, X., Yang, Y., and Wang, C. (2011) Observation of reduced cytotoxicity of aggregated amyloidogenic peptides with chaperone-like molecules. *ACS Nano 5*, 6001.
(79) Takai, E., Uda, K., Matsushita, S., Shikiya, Y., Yamada, Y., Shiraki, K., Zako, T., and Maeda, M. (2014) Cysteine inhibits amyloid fibrillation of lysozyme and directs the formation of small worm-like aggregates through non-covalent interactions. *Biotechnol. Prog. 30*, 470.
(80) Blennow, K., and Hampel, H. (2003) CSF markers for incipient Alzheimer's disease. *Lancet Neurol. 2*, 605.
(81) Blennow, K., Hampel, H., Weiner, M., and Zetterberg, H. (2010) Cerebrospinal fluid and plasma biomarkers in Alzheimer disease. *Nat. Rev. Neurol. 6*, 131.
(82) Seubert, P., Vigo-Pelfrey, C., Esch, F., Lee, M., Dovey, H., Davis, D., Sinha, S., Schlossmacher, M., Whaley, J., Swindlehurst, C., McCormack, R., Wolfert, R., Selkoe, D., Lieberburg, I., and Schenk, D. (1992) Isolation and quantification of soluble Alzheimer's β-peptide from biological fluids. *Nature 359*, 325.
(83) Dwivedi, A. K., and Iyer, P. K. (2014) Therapeutic strategies to prevent Alzheimer's disease pathogenesis using a fluorescent conjugated polyelectrolyte. *Macromol. Biosci. 14*, 508.
(84) Lee, J., Culyba, E. K., Powers, E. T., and Kelly, J. W. (2011) Amyloid-β forms fibrils by nucleated conformational conversion of oligomers. *Nat. Chem. Biol. 7*, 602.
(85) He, X., Park, H. M., Hyung, S. J., DeToma, A. S., Kim, C., Ruotolo, B. T., and Lim, M. H. (2012) Application of inorganic chemistry for non-cancer therapeutics. *Dalton Trans. 41*, 6558.
(86) Hindo, S. S., Mancino, A. M., Braymer, J. J., Liu, Y., Vivekanandan, S., Ramamoorthy, A., and Lim, M. H. (2009) Small molecule modulators of copper-induced Aβ aggregation. *J. Am. Chem. Soc. 131*, 16663.
(87) Jones, M. R., Service, E. L., Thompson, J. R., Wang, M. C. P., Kimsey, I. J., DeToma, A. S., Ramamoorthy, A., Lim, M. H., and Storr, T. (2012) Dual-function triazole−pyridine derivatives as inhibitors of metal-induced amyloid-β aggregation. *Metallomics 4*, 910.
(88) Choi, J., Braymer, J. J., Nanga, R. P. R., Ramamoorthy, A., and Lim, M. H. (2010) Design of small molecules that target metal-Aβ species and regulate metal-induced Aβ aggregation and neurotoxicity. *Proc. Natl. Acad. Sci. U. S. A. 107*, 21990.
(89) Hickey, J. L., Lim, S., Hayne, D. J., Paterson, B. M., White, J. M., Villemagne, V. L., Roselt, P., Binns, D., Cullinane, C., Jeffery, C. M., Price, R. I., Barnham, K. J., and Donnelly, P. S. (2013) Diagnostic imaging agents for Alzheimer's disease: Copper radiopharmaceuticals that target Aβ plaques. *J. Am. Chem. Soc. 135*, 16120.
(90) Cabaleiro-Lago, C., Quinlan-Pluck, F., Lynch, I., Lindman, S., Minogue, A. M., Thulin, E., Walsh, D. M., Dawson, K. A., and Linse, S. (2008) Inhibition of amyloid β protein fibrillation by polymeric nanoparticles. *J. Am. Chem. Soc. 130*, 15437.
(91) Cabaleiro-Lago, C., Szczepankiewicz, O., and Linse, S. (2012) The effect of nanoparticles on amyloid aggregation depends on the protein stability and intrinsic aggregation rate. *Langmuir 28*, 1852.
(92) Choi, I., and Lee, L. P. (2013) Rapid detection of Aβ aggregation and inhibition by dual functions of gold nanoplasmic particles: Catalytic activator and optical reporter. *ACS Nano 7*, 6268.
(93) Ridgley, D. M., Ebanks, K. C., and Barone, J. R. (2011) Peptide mixtures can self-assemble into large amyloid fibers of varying size and morphology. *Biomacromolecules 12*, 3770.
(94) Dehn, S., Castelletto, V., Hamley, I. W., and Perrier, S. (2012) Altering peptide fibrillization by polymer conjugation. *Biomacromolecules 13*, 2739.
(95) Nilsson, M. R., and Dobson, C. M. (2003) In vitro characterization of lactoferrin aggregation and amyloid formation. *Biochemistry 42*, 375.

DOI: 10.1021/acschemneuro.5b00205
ACS Chem. Neurosci. 2015, 6, 1880−1891

(96) del Mercato, L. L., Maruccio, G., Pompa, P. P., Bochicchio, B., Tamburro, A. M., Cingolani, R., and Rinaldi, R. (2008) Amyloid-like fibrils in elastin-related polypeptides: Structural characterization and elastic properties. *Biomacromolecules 9*, 796.
(97) Sharpe, S., Simonetti, K., Yau, J., and Walsh, P. (2011) Solid state NMR characterization of autofluorescent fibrils formed by the elastin-derived peptide GVGVAGVG. *Biomacromolecules 12*, 1546.
(98) Shirwany, N. A., Payette, D., Xie, J., and Guo, Q. (2007) The amyloid beta ion channel hypothesis of Alzheimer's disease. *Neuropsychiatr. Dis. Treat. 3*, 597.
(99) Takuma, K., Fang, F., Zhang, W., Yan, S., Fukuzaki, E., Du, H., Sosunov, A., McKhann, G., Funatsu, Y., Nakamichi, N., Nagai, T., Mizoguchi, H., Ibi, D., Hori, O., Ogawa, S., Stern, D. M., Yamada, K., and Yan, S. S. (2009) RAGE-mediated signaling contributes to intraneuronal transport of amyloid-β and neuronal dysfunction. *Proc. Natl. Acad. Sci. U. S. A. 106*, 20021.
(100) Agarwal, A., Covic, L., Sevigny, L. M., Kaneider, N. C., Lazarides, K., Azabdaftari, G., Sharifi, S., and Kuliopulos, A. (2008) Targeting a metalloprotease-PAR1 signaling system with cell-penetrating pepducins inhibits angiogenesis, ascites, and progression of ovarian cancer. *Mol. Cancer Ther. 7*, 2746.
(101) Rubin, L. L., Hall, D. E., Porter, S., Barbu, K., Cannon, C., Horner, H. C., Janatpour, M., Liaw, C. W., Manning, K., Morales, J., Tanner, L. I., Tomaselli, K. J., and Bard, F. (1991) A Cell Culture Model of the Blood-Brain Barrier. *J. Cell Biol. 115*, 1725.

DOI: 10.1021/acschemneuro.5b00205
ACS Chem. Neurosci. 2015, 6, 1880−1891